

Sex-specific differences in direct osteoclastic *versus* indirect osteoblastic effects underlay the low bone mass of Pannexin1 deletion in TRAP-expressing cells in mice

Padmini Deosthale^{a,b}, Jung Min Hong^c, Alyson L. Essex^{a,b,d}, Wilyaret Rodriguez^a, Dua Tariq^a, Harmandeep Sidhu^a, Alejandro Marcial^a, Angela Bruzzaniti^{c,d}, Lilian I. Plotkin^{a,b,d,*}

^a Department of Anatomy, Cell Biology & Physiology, Indiana University School of Medicine, USA

^b Roudebush Veterans Administration Medical Center, USA

^c Department of Biomedical Sciences and Comprehensive Care, Indiana University School of Dentistry, USA

^d Indiana Center for Musculoskeletal Health, Indianapolis, IN, USA

ARTICLE INFO

Keywords:

Osteoclast

Pannexin

Bone mass

Bone resorption

ABSTRACT

Pannexin1 (Panx1) is a hemichannel-forming protein that participates in the communication of cells with the extracellular space. To characterize the role of osteoclastic Panx1 on bone, Panx1^{fl/fl};TRAP-Cre (Panx1^{ΔOc}) mice were generated, and compared to Panx1^{fl/fl} littermates at 6 weeks of age. Total and femoral BMD was ~20% lower in females and males whereas spinal BMD was lower only in female Panx1^{ΔOc} mice. μ CT analyses showed that cortical bone of the femoral mid-diaphysis was not altered in Panx1^{ΔOc} mice. In contrast, cancellous bone in the distal femur and lumbar vertebra was significantly decreased in both female and male Panx1^{ΔOc} mice compared to Panx1^{fl/fl} controls and was associated with higher osteoclast activity in female Panx1^{ΔOc} mice, with no changes in the males. On the other hand, vertebral bone formation was decreased for both sexes, resulting from lower mineral apposition rate in the females and lower mineralizing surface in the males. Consistent with an osteoclastic effect in female Panx1^{ΔOc} mice, osteoclast differentiation with RANKL/M-CSF and osteoclast bone resorbing activity *in vitro* were higher in female, but not male, Panx1^{ΔOc} mice, compared to Panx1^{fl/fl} littermates. Surprisingly, although Panx1 expression was normal in bone marrow stromal-derived osteoblasts from male and female Panx1^{ΔOc} mice, mineral deposition by male (but not female) Panx1^{ΔOc} osteoblasts was lower than controls, and it was reduced in male Panx1^{fl/fl} osteoblasts when conditioned media prepared from male Panx1^{ΔOc} osteoclast cultures was added to the cell culture media. Thus, deletion of Panx1 in TRAP-expressing cells in female mice leads to low bone mass primarily through a cell autonomous effect in osteoclast activity. In contrast, our evidence suggests that changes in the osteoclast secretome drive reduced osteoblast function in male Panx1^{ΔOc} mice, resulting in low bone mass.

1. Introduction

Pannexins are glycoproteins that form channels in the plasma membrane allowing the exchange of small molecules between the cells and the extracellular space (Beyer and Berthoud, 2018). Pannexin channels exhibit aminoacid sequence analogy to invertebrate innexins and are structurally and topologically similar to connexins, but without sharing sequence homology. Yet, unlike connexins, pannexin channels do not connect with channels in other cells and therefore, do not mediate direct cell-to-cell communication. Rather, pannexins release signaling

molecules extracellularly. Three different pannexins have been identified, 1, 2, and 3, with pannexin 1 (Panx1) being the most abundant and most studied member of the family. Dysregulation of Panx1 function has been associated with several pathologies, including inflammation, cancer, and cardiovascular disease. Further, Panx1 is expressed in all bone cells and in skeletal muscle (Plotkin et al., 2017), and deletion of Panx1 from osteocytic cells results in increased bone mass in female mice assessed at 4 and 13 months of age (Aguilar-Perez et al., 2019). In addition, osteocytic Panx1 deletion leads to increased skeletal muscle mass in female mice but decreased skeletal muscle strength in male

* Corresponding author at: Department of Anatomy, Cell Biology & Physiology, Indiana University School of Medicine, 635 Barnhill Drive, MS-5035, Indianapolis, IN 46202-5120, USA.

E-mail address: lplotkin@iupui.edu (L.I. Plotkin).

<https://doi.org/10.1016/j.bonr.2021.101164>

Received 27 October 2021; Received in revised form 17 December 2021; Accepted 27 December 2021

Available online 4 January 2022

2352-1872/© 2022 The Authors.

Published by Elsevier Inc.

This is an open access article under the CC BY-NC-ND license

(<http://creativecommons.org/licenses/by-nc-nd/4.0/>).

mice. Thus, the effect of osteocytic Panx1 deletion in the musculoskeletal system is sex dependent. However, whether Panx1 in other bone cells such as osteoclasts is similarly regulated in a sex-dependent manner remains unknown.

Bone accrual during development depends on the function of bone forming osteoblasts and bone resorbing osteoclasts (Bellido et al., 2019). Previous studies showed that inhibition of Panx1 channels using mefloquine or small molecule analogs have pro- or anti-osteoclast differentiation effects *in vitro*, depending on the inhibitor dose and the age of the mice (Pacheco-Costa et al., 2018). However, because of the lack of specificity of these pharmacological inhibitors, it was not possible to conclusively determine whether Panx1 has a role in osteoclast differentiation. Therefore, to establish the role of Panx1 in osteoclasts, we generated mice in which PANX1 expression was deleted from osteoclastic cells by mating mice expressing the floxed Panx1 gene (Panx1^{fl/fl}) (Aguilar-Perez et al., 2019) with TRAP-Cre mice, expressing the Cre recombinase under the control of the tartrate-resistance acid phosphatase (TRAP) promoter (Chiu et al., 2004) named Panx1^{ΔOc}. The skeletal phenotype of the Panx1^{ΔOc} mice was analyzed at 6 weeks of age, to determine the bone phenotype prior to skeletal maturation, which typically occurs at 16 weeks of age in mice of the C57BL/6 background strain.

We report herein that osteoclastic Panx1 deletion results in decreased bone mass in both male and female 6-week-old mice. However, whereas female mice exhibit increased osteoclast activity *in vivo* and *in vitro*, and decreased bone formation *in vivo*, male mice show no change in osteoclasts, and a reduction of both bone formation *in vivo* and osteoblastic cell mineralization *ex vivo*.

2. Materials and methods

2.1. Animals

Mice expressing the floxed Panx1 gene (Panx1^{fl/fl}), previously reported (Aguilar-Perez et al., 2019), were mated with TRAP-Cre mice, expressing the Cre recombinase under the control of the TRAP promoter (Chiu et al., 2004), to generate mice lacking Panx1 in osteoclasts (Panx1^{ΔOc}) and Panx1^{fl/fl} littermate controls. Mice were genotyped for expression of the floxed Panx1 gene using Transnetyx genotyping services. PCR for TRAP-Cre transgene was performed using the following primer set: Cre1-Forward: GAGTGATGAGGTTGCAAGA, Cre2-Reverse: CTACACCAGAGACGGAATC.

To confirm Panx1 deletion in osteoclasts, but not in cells of the osteoblastic lineage, we isolated total bone marrow cells and cultured them for 48 h. Adherent cells containing bone marrow stromal cells (BMSC) were separated from non-adherent bone marrow cells containing osteoclast precursors. Osteoclast formation was induced as detailed below and DNA was collected 4 days after adding RANKL and M-CSF. DNA was extracted from both osteoclasts and stromal cells using the Purelink Genomic DNA Mini kit (Invitrogen, cat#K1820-02). The presence of floxed Panx1 gene, and the deleted form of the gene (generated as a consequence of TRAP-Cre recombinase activity) was determined using KAPA Taq ReadyMix (Kapa Biosystems Pty Ltd., cat#KK1024) and the following primers: LoxP1-F: TGAATGCAATTGTTGTTTAAC; LoxP2-F: CTTATCATGTCTGGATCCGG; and LoxP3-R GACAGGAATATAGCAGGTATC. The thermal cycling parameters were 95 °C for 3 min, 38 cycles of (95 °C for 15 s, 53.6 °C for 15 s, 72 °C for 15 s) and final extension at 72 °C for 2 min. A band at 1092 bp signified no deletion, and a band at 339 bp signified a deletion of the floxed Panx1 gene.

Blood was collected from the facial vein of 6-week-old mice after 5 h of fasting. Serum was separated using BD microcontainer tubes, aliquoted, and stored at -80 °C. The levels of CTX-I were measured using the RatLaps™ EIA kit (IDS, Scottsdale, AZ, USA) according to manufacturer's instructions.

Mice were maintained on regular diet and water *ad libitum*. All

animal procedures were approved by the IUSM IACUC, and animal care and studies were carried out in accordance with institutional guidelines.

2.2. Bone mineral density

Bone mineral density (BMD) measurements were performed following previously published procedures using a Dxa/Piximus instrument (Aguilar-Perez et al., 2019; Davis et al., 2020) after phantom calibration, as per the manufacturer's instruction. Total (whole body, excluding the head and tail), femoral (whole femur) and spinal (lumbar vertebrae L1 to L6) BMD were measured.

2.3. μ CT analyses

Femur and lumbar vertebrae (L5) were dissected, wrapped in a saline-containing gauze and kept at -20 °C until scanned. Bones were scanned as previously published using a Skyscan 1176 system (65 kV source, 0.5 mm Al filter, 0.7-degree rotation, two-image averaging and isotropic voxel of 9 μ m) (Aguilar-Perez et al., 2019). The terminology and units follow the standards for the field (Bouxsein et al., 2010).

Representative data sets of cortical bone at the mid-diaphysis and distal cancellous bone in the femora, and cancellous bone of L5 vertebrae were selected for 3D rendering. To obtain standardized rendered figures, the data sets were uploaded to a high-performance imaging analysis software, DRAGONFLY (Version 2021.3.0.1069, Object Research Systems, Canada). All Volumes of Interest (VOIs) from the data sets were rendered following an automatic segmentation protocol within the software, based on the Otsu method for thresholding (Otsu, 1979). Then, 3D surface meshes were generated for each representative bone sample.

2.4. Histomorphometry

Animals were injected intraperitoneally with 30 mg/kg calcein and 50 mg/kg alizarin 7 and 2 days before sacrifice, respectively, for dynamic histomorphometric measurements (Davis et al., 2018). Lumbar vertebrae (L1–L3) were isolated and fixed in 10% neutral buffered formalin and embedded in methyl-methacrylate. Histomorphometric analysis was performed using the Osteomeasure high resolution digital video system software (Osteometrics Inc., Decatur, GA, USA). Osteoblast and osteoclast parameters were scored in von-Kossa/McNeal- and TRAP/Toluidine blue-stained vertebral bone sections, respectively. Dynamic measurements were performed on unstained sections. Images were taken using an Olympus BX51 fluorescent microscope and Olympus cellSense Entry 1.2 (Build 7533) imaging software. The terminology and units follow the ASBMR Histomorphometry Nomenclature Committee guidance (Dempster et al., 2013). All histological procedures were performed at the Histology and Histomorphometry Laboratory (ACBP, ICMH, Indiana CTSI) at Indiana University School of Medicine.

2.5. Cell culture

2.5.1. Osteoclast cultures

Bone marrow cells were collected from 6-week-old femurs and tibiae by cutting the ends of the bones and flushing the cells out with 10% FBS/1% penicillin/streptomycin (P/S)-containing α -MEM media. Bone marrow cells were cultured for 48 h, as previously published (Davis et al., 2017). Subsequently, non-adherent cells containing hematopoietic cells, including osteoclast precursors were separated from adherent cells, which include stromal cells that can differentiate into osteoblastic cells.

Bone marrow non-adherent cells were cultured in the presence of 30 ng/ml macrophage colony stimulating factor (M-CSF) for 3 days, to estimate the effect of Panx1 deletion on the number of viable precursor cell, as previously reported (Posritong et al., 2018; Wu et al., 2020). The

media was then replaced with 100 μ l fresh medium containing 20 μ l of CellTiter 96 AQueous One Solution (CellTiter 96® AQueous Non-Radioactive Cell Proliferation Assay (MTS) kit, Promega, Madison, WI). Cells were incubated at 37 °C for 3 h and cell viability was estimated by measuring the optical density (OD) at 490 nm (Mohamad et al., 2021). To minimize the contribution of estrogen, phenol-free α MEM media and charcoal-stripped FBS (Biowest) were used in a separate experiment.

For osteoclast differentiation, bone marrow non-adherent cells were seeded at a density of $1.5 \times 10^5/\text{cm}^2$ and differentiated in α -MEM containing 10% FBS, 1% P/S with 80 ng/ml receptor activator of NF κ B ligand (RANKL) and 20 ng/ml M-CSF (Davis et al., 2019a). After 4 or 5 days of osteoclast differentiation, cells were fixed with 10% neutral buffered formalin and stained for TRAP using an Acid Phosphatase, Leukocyte kit (Sigma Aldrich; cat.# 387A). Mature osteoclasts were identified as cells with 3 or more nuclei. Cells were counted using an inverted brightfield Leica DMI 4000 B microscope and osteoclast size was quantified using the ImagePro software (Media Cybernetics, Inc., Rockville, MS, USA).

Conditioned media (CM) was collected from non-adherent cells seeded at density $4.5 \times 10^5/\text{cm}^2$, 4 days after addition of RANKL and M-CSF as above. CM was stored at -80 °C until used.

To measure osteoclastic activity Panx1^{fl/fl} and Panx1^{ΔOc} osteoclasts were generated from bone marrow non-adherent cells as detailed above and cultured for 5 days. Cells were then detached with trypsin-EDTA and gentle scraping, as previously published by us (Kang et al., 2019). The detached mature osteoclasts were washed with complete media, and an identical number of cells were reseeded onto cortical bone slices (approx. 200 osteoclasts per slice in 96 well plates) and cultured for 3 additional days (Mohamad et al., 2017). Culture media were collected from the bone slices, and CTX-I levels were measured using a CrossLaps® for Culture ELISA kit (IDS, Scottsdale, AZ, USA). Cells on the bone slices were also stained for TRAP as indicated above and enumerated, and the levels of CTX-I in the media were corrected by the number of mature TRAP-positive osteoclasts. For osteoclast pit staining on cortical bone slices, the osteoclasts were removed by mechanical agitation, and the bone slices were incubated with 20 μ g/ml peroxidase-conjugated wheat germ agglutinin for 1 h. After washing with PBS, 3,3'-diaminobenzidine (Sigma-Aldrich) was added, and the pits were imaged using an inverted brightfield Leica DMI 4000 B microscope. The pit area was measured using the Image Pro software (Media Cybernetics, Inc., Rockville, MS, USA).

2.5.2. Osteoblastogenesis assays

Bone marrow cells were cultured for 48 h as above. Non-adherent cells were removed, and adherent cells (bone marrow stromal cells) were trypsinized and re-seeded at density $4 \times 10^5/\text{cm}^2$ for mineralization analysis, and at $4 \times 10^6/\text{cm}^2$ for RNA isolation. Cells were cultured in the presence of 5 mM of β -glycerolphosphate and 25 μ g/ml ascorbic acid (osteoblastogenic media) to induce osteoblast differentiation. To test for effect of osteoclast CM on osteoblast differentiation/activity, 10% CM in osteoblastogenic media was added from day 1 to the adherent cells obtained from mice of the same sex, seeded at density $4 \times 10^5/\text{cm}^2$. Media was changed every 2–3 days and fresh CM and osteoblastogenic media were added.

After 14 days of culture, cells were fixed and the mineral deposited was stained using 40 mM alizarin red S (Sigma Aldrich; cat.#A5533) as previously published (Davis et al., 2019b). The deposited stain was extracted with 1% cetylpyridinium chloride for 15 min and absorbance was measured at 490 nm (Davis et al., 2019b). Proteins were extracted from the remaining cells using a lysis buffer containing 20 mM Tris-HCl, pH 7.5, 150 mM NaCl, 1 mM EDTA, and 1% Triton X100, supplemented with 2 μ g/ml aprotinin, 5 μ g/ml leupeptin, 10 mM NaF, 1 mM Na₃VO₄, 1 mM phenyl methyl sulfonyl fluoride (PMSF) and Halt Protease Inhibitor Cocktail (Thermo Fisher Scientific Inc., Rockford, IL, USA, cat.#78430) (Aguilar-Perez et al., 2019). Protein concentration was measured using a

Pierce BCA Protein Assay Kit (Thermo Scientific, cat.#23225). Data is reported as optical density at 490 nm (OD)/protein concentration for each well (Li et al., 2020).

2.6. RNA extraction and gene expression

RNA was isolated using Trizol (Invitrogen) as previously published (Davis et al., 2017). Reverse transcription was performed using the high-capacity cDNA transcription kit (Applied Biosystems, Invitrogen, Foster City, CA, USA). Quantitative PCR (qPCR) was performed using the Fast Taqman Universal PCR Mastermix in a Step One Plus real time PCR instrument (Applied Biosystems). Gene expression levels were normalized using the housekeeping gene glyceraldehyde-3 phosphate dehydrogenase (GAPDH). Primers and probes were available commercially (Applied Biosystems) or were designed using the Assay Design Center (Roche Applied Sciences). Relative expression was calculated using $\Delta\Delta C_t$ comparative method (Livak and Schmittgen, 2001).

2.7. Western blot analysis

Protein lysates from osteoclasts generated four days after addition of RANKL and M-CSF were prepared in lysis buffer, as previously described (Aguilar-Perez et al., 2019). Cell lysate protein content was quantified using a Pierce BCA Protein Assay Kit (Thermo Scientific, cat.#23225) according to manufacturer's instructions. Protein lysates (22 μ g/line) and Precision Plus Protein™ WesternC™ Standards molecular weight markers (Bio-Rad; cat.#161-0376) were separated on BioRad AnyKD (50 μ l) gels and transferred to PVDF membrane using a Bio-Rad transfer system. The membranes were cut at the 75kD mark using the MWM ladder as reference. The membranes were incubated in blocking solution (0.5% skim milk-TBST solution) for 1 h on a rocker at room temperature, followed by addition of mouse monoclonal anti- β -actin (Sigma; cat.#A5316; 1:5000) or purified mouse monoclonal anti- β -catenin (BD Transduction Laboratories™; cat.#610153; 1:750) antibodies overnight on a rocker at 4 °C. Goat anti-mouse-horseradish peroxidase (HRP) secondary antibody (EMD Millipore Corp; cat.#71045-3) was used at a 1:5000 dilution for β -actin and 1:3000 for β -catenin. The StrepTactin-HRP conjugate was added to the secondary antibody solutions for detection of the molecular weight markers (Precision Protein™; Bio-Rad; cat.#1610381; 1:15000). The membranes were probed with the secondary antibodies for 2.5 h at room temperature on a shaker. After washing three times in TBS-T and once in TBS buffer, a chemiluminescence substrate (Pierce™ ECL Western Blotting Substrate; Thermo Scientific; cat.#32106) was added and kept for 5 min on a rocker at room temperature. The membranes were exposed for 1 and 2 min to reveal the β -actin (55kD) and β -catenin (95kD) bands, respectively, using a ChemiDoc™ Imaging System (Bio-Rad; S/N: 733BR2682). The intensity of the bands was quantified using ImageJ.

2.8. Statistical analysis

The data was analyzed using SigmaPlot (Systat Software, Inc., San Jose, CA, USA), Normal distribution was established using the Shapiro-Wilk Normality Test, and equal variance by the Brown-Forsythe test. Difference between groups was established using unpaired 2-tailed Student's *t*-test (for normally distributed values) or the Mann-Whitney Rank Sum test (for data that was not normally distributed). Values are reported as mean \pm standard deviation. Differences with *p* < 0.05 were considered statistically significant.

3. Results

3.1. Deletion of osteoclastic Panx1 results in low bone mass in male and female mice

Cre recombinase was effectively targeted to osteoclastic cells and not

to cells of the osteoblastic lineage, as demonstrated by the presence of the deleted form of the *Panx1* gene in osteoclast cultures, but not in bone marrow stromal cell (BMSC) preparations (Fig. 1A). Both female and male mice lacking *Panx1* from osteoclasts ($Panx1^{\Delta Oc}$) exhibit significantly lower total and femoral BMD, whereas lumbar spinal BMD was only reduced in female mice at 1 month of age, compared to $Panx1^{fl/fl}$ littermates (Fig. 1B). We did not find differences in body weight or lean body mass for either sex, but fat mass was lower only in male $Panx1$ -deficient mice compared to littermate control mice at this age (Fig. 1C). Subsequent studies were performed in 6-week-old mice.

3.2. Lack of *Panx1* in osteoclasts specifically reduces cancellous bone without altering cortical bone structure

Micro-CT studies of male and female $Panx1^{\Delta Oc}$ and $Panx1^{fl/fl}$ controls were performed in 6-week-old mice. Deletion of *Panx1* from osteoclastic cells leads to a decrease in trabecular number in the lumbar vertebrae and the distal femur for both sexes (Fig. 2). Trabecular separation was only increased in cancellous bone of the lumbar vertebra in female mice (Fig. 2A), and bone volume was lower, and trabecular separation was higher compared to control littermates in the distal femur of male mice (Fig. 2B). Tendencies towards decreased bone volume were also found in

cancellous bone in the distal femur and the vertebra for male and female $Panx1^{\Delta Oc}$ mice, respectively (Fig. 2). In contrast, despite a decrease in BMD, deletion of *Panx1* from osteoclastic cells did not affect cortical bone geometry or bone mass in the femoral mid-diaphysis for either female or male mice (Fig. 3).

3.3. *Panx1* deletion differentially affects osteoblasts and osteoclasts in female and male $Panx1^{\Delta Oc}$ mice

Histomorphometric analysis of the cancellous bone of the lumbar vertebra showed increased osteoclast-related parameters in female mice, with approximately 2-fold higher osteoclast surface and number and eroded surface (Fig. 4A). On the other hand, no changes were observed in osteoclastic parameters in male mice. Consistent with this, deletion of osteoclastic *Panx1* resulted in significantly higher circulating levels of CTX-I in female $Panx1^{\Delta Oc}$ mice (66.04 ± 17.21 ng/ml) compared to female $Panx1^{fl/fl}$ mice (43.94 ± 17.11 ng/ml), whereas circulating CTX-I was similar between $Panx1^{\Delta Oc}$ (125.74 ± 44.67 ng/ml) and $Panx1^{fl/fl}$ (142.66 ± 39.19 ng/ml) male mice.

The number of osteoblasts was significantly lower in both female and males, whereas osteoid volume was only lower in male $Panx1$ -deficient mice, with a tendency towards lower values in osteoblast surface and

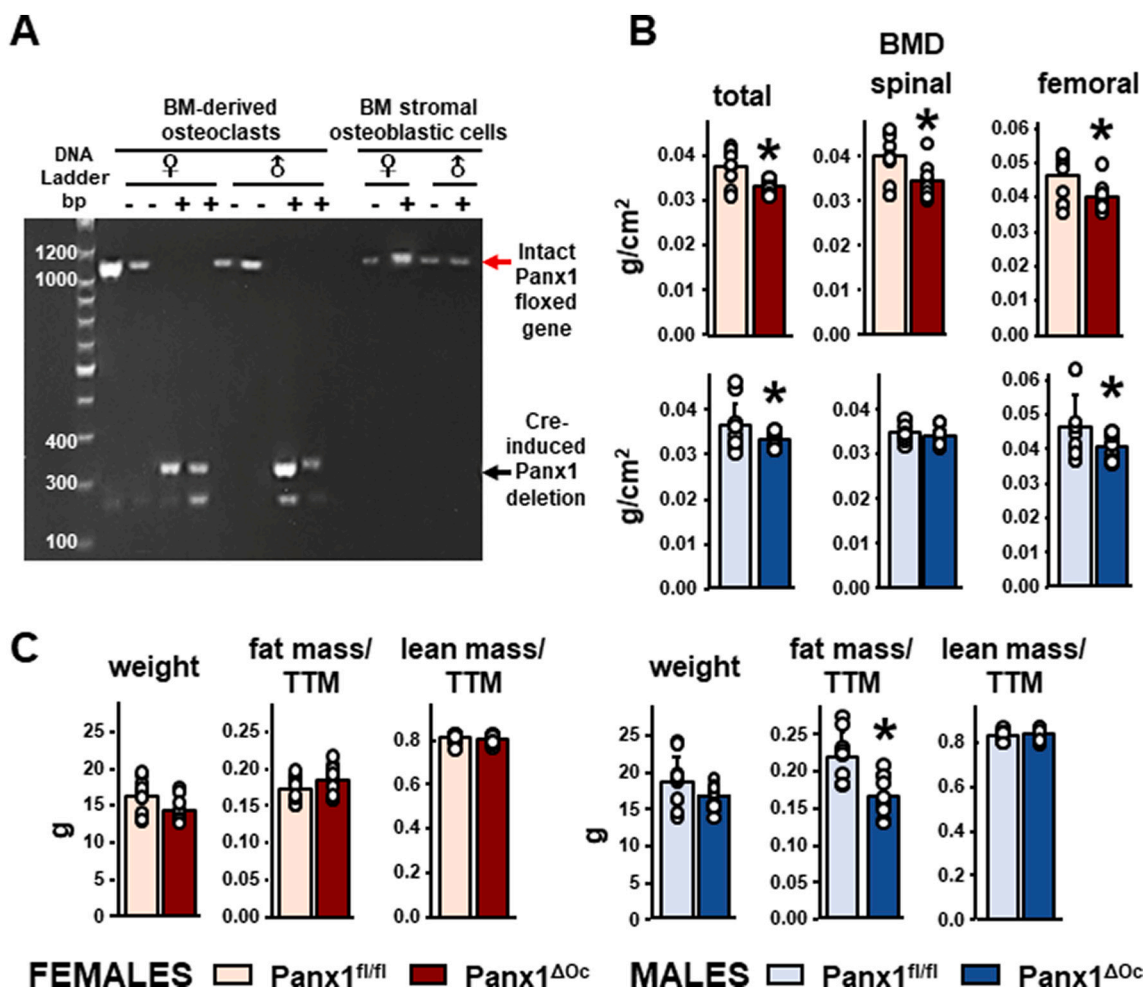


Fig. 1. Low bone mass in mice lacking *Panx1* in osteoclasts. A. Presence of the deleted *Panx1* form was detected by PCR. Each lane corresponds to an individual female or male $Panx1^{fl/fl}$ animal expressing (+) or not (-) the Cre recombinase under the control of the TRAP promoter. The first lane corresponds to a DNA ladder, and selected DNA sizes (base pairs, bp) are marked. Red arrow points at the expected size for the intact *Panx1* gene (1092 bp), and the black arrow, the size of the gene after deletion (339 bp). BM-derived osteoclasts: non-adherent cells treated with RANKL/MCSF for 4 days; BM stromal osteoblastic cells: bone marrow-derived adherent cells; ♀: females; ♂: males. B. Total, spinal, and femoral BMD were measured by Dxa/Piximus in female and male $Panx1^{\Delta Oc}$ mice and $Panx1^{fl/fl}$ mice at 4 weeks of age. C. Body weight measured at the time of Dxa measurement, and lean and fat body mass calculated from the Dxa scan of the same mice. $N = 11-12/\text{group}$. Bars indicate means and lines standard deviations, and each dot corresponds to an individual sample. *: $p < 0.05$ vs. $Panx1^{fl/fl}$ mice for the same sex.

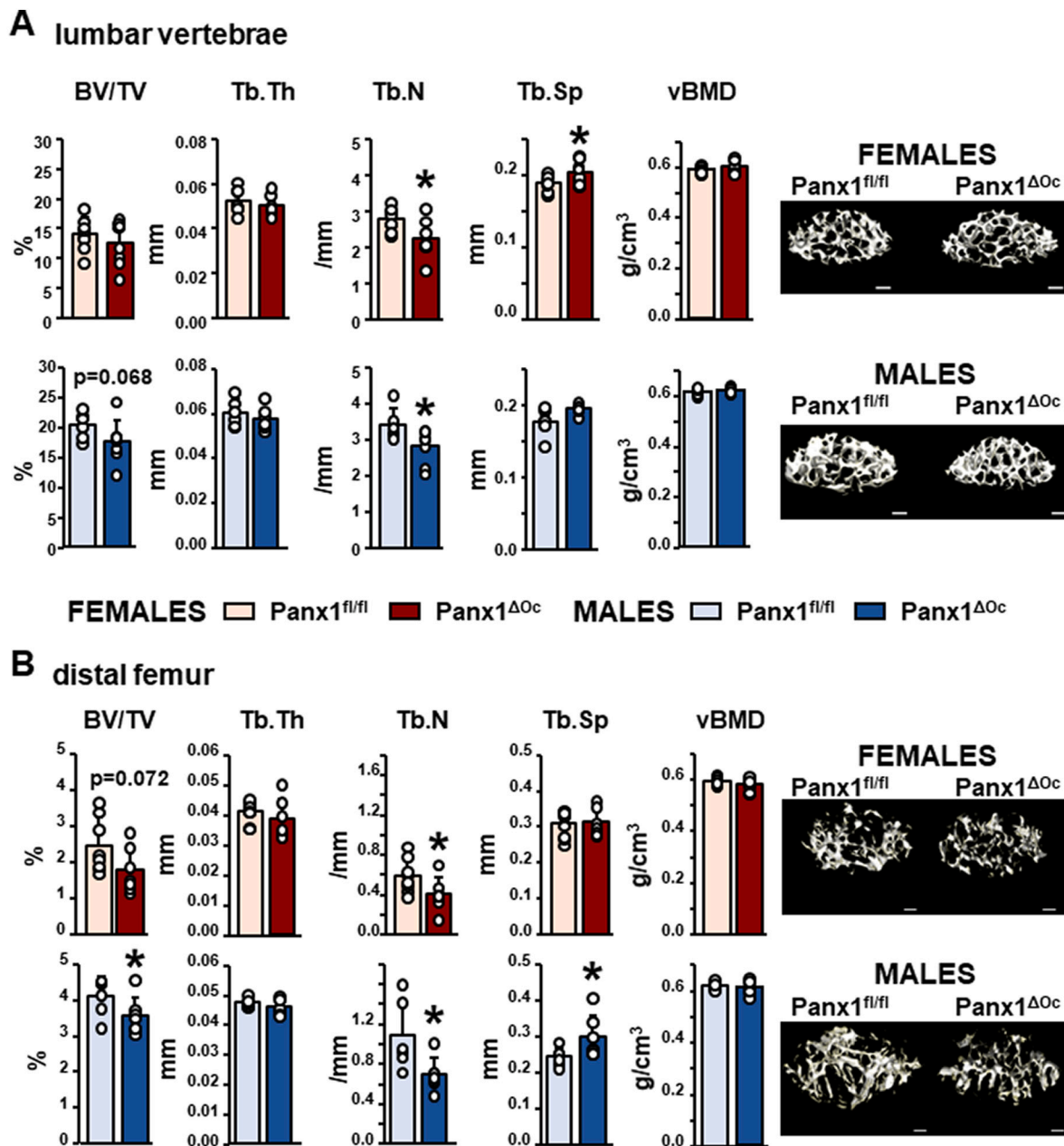


Fig. 2. Reduced cancellous bone mass in mice lacking Panx1 in osteoclastic cells. μ CT analyses were performed in the fifth lumbar vertebrae (A) and distal femur (B) from female and male Panx1^{ΔOc} mice and Panx1^{fl/fl} mice at 6 weeks of age. *N* = 6–8/group. Bars indicate means and lines standard deviations, and each dot corresponds to an individual sample. *: *p* < 0.05 vs. Panx1^{fl/fl} mice for the same sex. Representative μ CT images for both sites are shown, scale bar corresponds to 0.25 mm.

osteoid volume in the females (Fig. 4B). Bone formation rate as measured by dynamic histomorphometry was lower for both female and male Panx1^{ΔOc} mice, compared to Panx1^{fl/fl} littermates (Fig. 4C). The lower bone formation observed in Panx1^{ΔOc} females was associated with reduced mineral apposition rate. In contrast, Panx1^{ΔOc} males showed reduced mineralizing surface. Together, these data suggest that different mechanisms contribute to the reduced bone formation of Panx1^{ΔOc} mice, depending on the sex of the animals.

3.4. Lack of Panx1 in female Panx1^{ΔOc} results in increased osteoclastic bone resorption

We next examined whether Panx1^{ΔOc} mice exhibit cell autonomous effects on osteoclastogenesis and bone resorption, and whether these

effects were sex specific. As expected, the levels of Panx1 were similar in females and males at the time of seeding the bone marrow cells (day 0) but were reduced by 50% after 4 days in culture (Fig. 5A). In spite similar reduction in Panx1 levels, the expression of the M-CSF receptor, CSF1R, and the transcription factor c-Fos was significantly higher in osteoclasts from female mice at day 4, whereas CSF1R was not different and c-Fos showed a tendency towards increase in osteoclastic cells derived from Panx1^{ΔOc} males (Fig. 5B). Further, only cells isolated from female Panx1^{ΔOc} mice exhibit an increased ability to differentiate into osteoclasts, resulting in higher osteoclast number and area (Fig. 5C and D). In addition, osteoclasts derived from Panx1^{ΔOc} females exhibited higher bone resorbing activity than cells isolated from control littermates, as evidenced by the increased release of CTX-I to the media (a measurement of resorptive activity), and by the larger area resorbed,

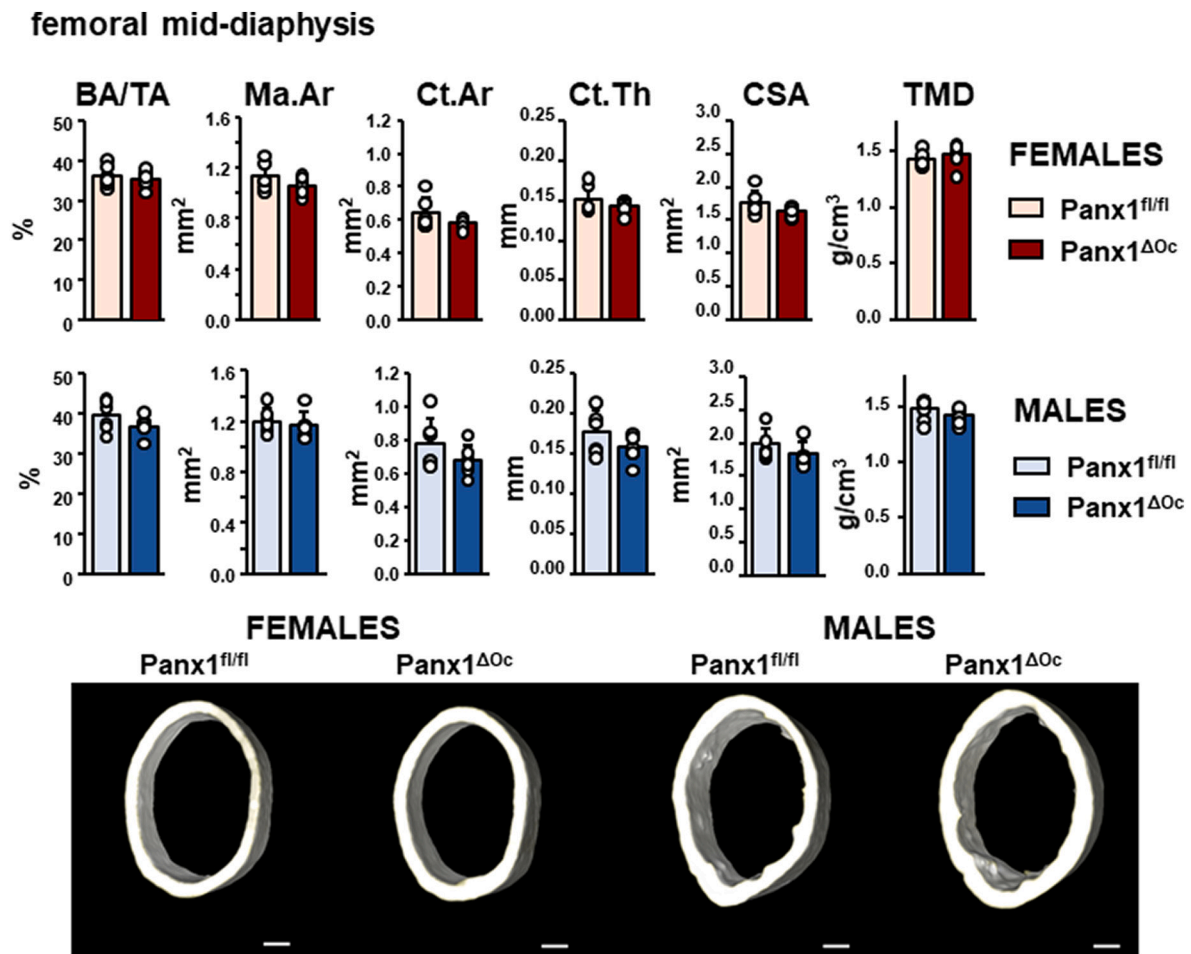


Fig. 3. Deletion of Panx1 from osteoclasts does not alter cortical bone in the femoral mid-diaphysis. μ CT analyses showed no differences in any parameter measured in female or male femoral bones at 6 weeks of age. $N = 6-7/\text{group}$. Bars indicate means and lines standard deviations, and each dot corresponds to an individual sample. Representative μ CT images are shown, scale bar corresponds to 0.25 mm.

resulting in bigger pits (Fig. 5E).

Further, proliferation of undifferentiated bone marrow cells was higher in cells isolated from female mice and lower in cells isolated from male mice, compared to control littermates (Fig. 5F). To rule out a potential contribution of estrogenic effects of compounds present in the culture media, cells were cultured in phenol-free α MEM containing 10% charcoal-stripped FBS, resulting in similar changes as complete media. This suggests that the difference in cell proliferation does not result from different sensitivity to estrogenic compounds in cells derived from Panx1^{ΔOc} versus Panx1^{fl/fl} mice.

Another potential difference in cells from Panx1-deficient mice and Panx1-expressing controls is the activation of the Wnt/ β catenin signaling. Indeed, previous studies have shown that Panx1 binds to β catenin in melanoma cells and that β catenin levels are decreased when Panx1 is knocked down (Sayed-yahosseini et al., 2021). Based on this evidence, and the fact that activation of the Wnt/ β catenin signaling pathway has been shown to modulate osteoclast differentiation (Kobayashi et al., 2015; Weivoda et al., 2016), we examined whether osteoclasts from Panx1^{ΔOc} mice exhibit changes in β catenin protein levels. β -catenin levels were similar in osteoclasts derived from Panx1^{ΔOc} female mice but were approximately 40% higher in osteoclasts derived from Panx1^{ΔOc} males, compared to cells from Panx1^{fl/fl} controls (Fig. 6). Taken together, these results suggest that the differences in osteoclast differentiation and activity between Panx1-deficient and Panx1-expressing osteoclasts does not depend on differential activation of canonical Wnt signaling.

We also found higher expression of osteoclast-related genes in

lumbar vertebrae from female Panx1^{ΔOc} mice compared to Panx1^{fl/fl} of the same sex (Fig. 7). On the other hand, only TRAP, and to a lesser extent NFATc1 were higher in bone preparations from male Panx1-deficient mice.

3.5. Decreased mineralization of bone marrow cells obtained from male, but not female, Panx1^{ΔOc} mice

To determine the cellular mechanism for the reduced bone mass in male mice, we examined whether deletion of osteoclastic Panx1 has an indirect effect on osteoblastic cells. We found similar levels of mineralization in cells isolated from Panx1^{fl/fl} and Panx1^{ΔOc} female mice (Fig. 8A). On the other hand, stromal osteoblastic cells from male Panx1^{ΔOc} mice exhibit lower capacity to mineralize, compared to cells from Panx1^{fl/fl} mice. We then tested whether the observed effect on mineral deposition was due to products released by Panx1^{ΔOc} osteoclastic cells. No differences in alizarin red staining were detected when osteoblast progenitors from female mice were exposed to CM from female Panx1^{fl/fl} or Panx1^{ΔOc} osteoclasts (Fig. 8B). In contrast, CM from male Panx1^{ΔOc} osteoclasts inhibit osteoblast mineralization, independently of whether the osteoblast precursors were isolated from Panx1^{fl/fl} or Panx1^{ΔOc} male mice. Moreover, CM from Panx1^{fl/fl} male osteoclasts reversed the lower mineralization potential of bone marrow stromal cells isolated from Panx1^{ΔOc} mice of the same sex, suggesting that in the absence of Panx1, osteoclasts are not able to release molecule(s) able to stimulate osteoblast differentiation. As expected, Panx1 levels were unchanged in stromal/osteoblastic cells from female or male Panx1^{ΔOc} mice compared

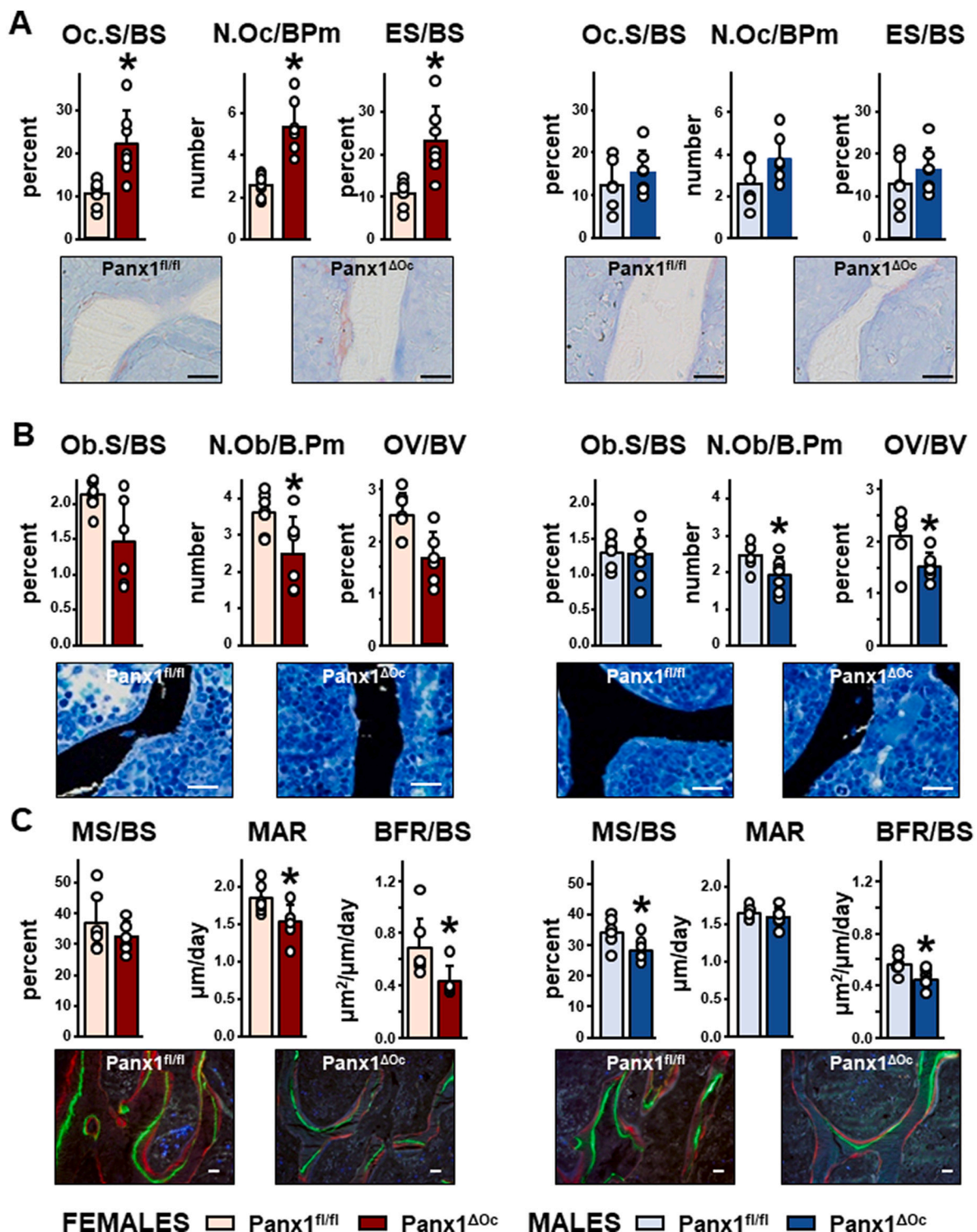


Fig. 4. Deletion of osteoclastic Panx1 results in higher osteoclastic parameters only in female mice. Static (A and B) and dynamic (C) histomorphometric parameters in cancellous bone of the second lumbar vertebrae of female and male mice at 6 weeks of age. N = 6–7/group. Bars indicate means and lines standard deviations, and each dot corresponds to an individual sample. *: p < 0.05 vs. Panx1^{fl/fl} mice for the same sex. Representative images are shown under the graphs. Scale bar = 20 μm.

to Panx1^{fl/fl} littermates after 14 day-treatment with osteoblastogenic media (Fig. 8C). However, consistent with the decreased osteoblast mineralization, the expression of DMP1 and Phex, two genes associated with the regulation of phosphate metabolism (Plotkin and Bellido, 2016), were lower in the osteoblastic cells derived from Panx1^{ΔOc} males and remained unchanged in cells from female animals. On the other hand, the levels of E11, a gene expressed in early osteocytes, was higher

in osteoblastic cells from Panx1^{ΔOc} male mice. Further, male Panx1^{ΔOc} exhibit higher levels of Sost, the gene that encodes for the bone formation inhibitor sclerostin, in vertebral bone whereas the level of the gene was not changed in bones from female mice (Fig. 8D).

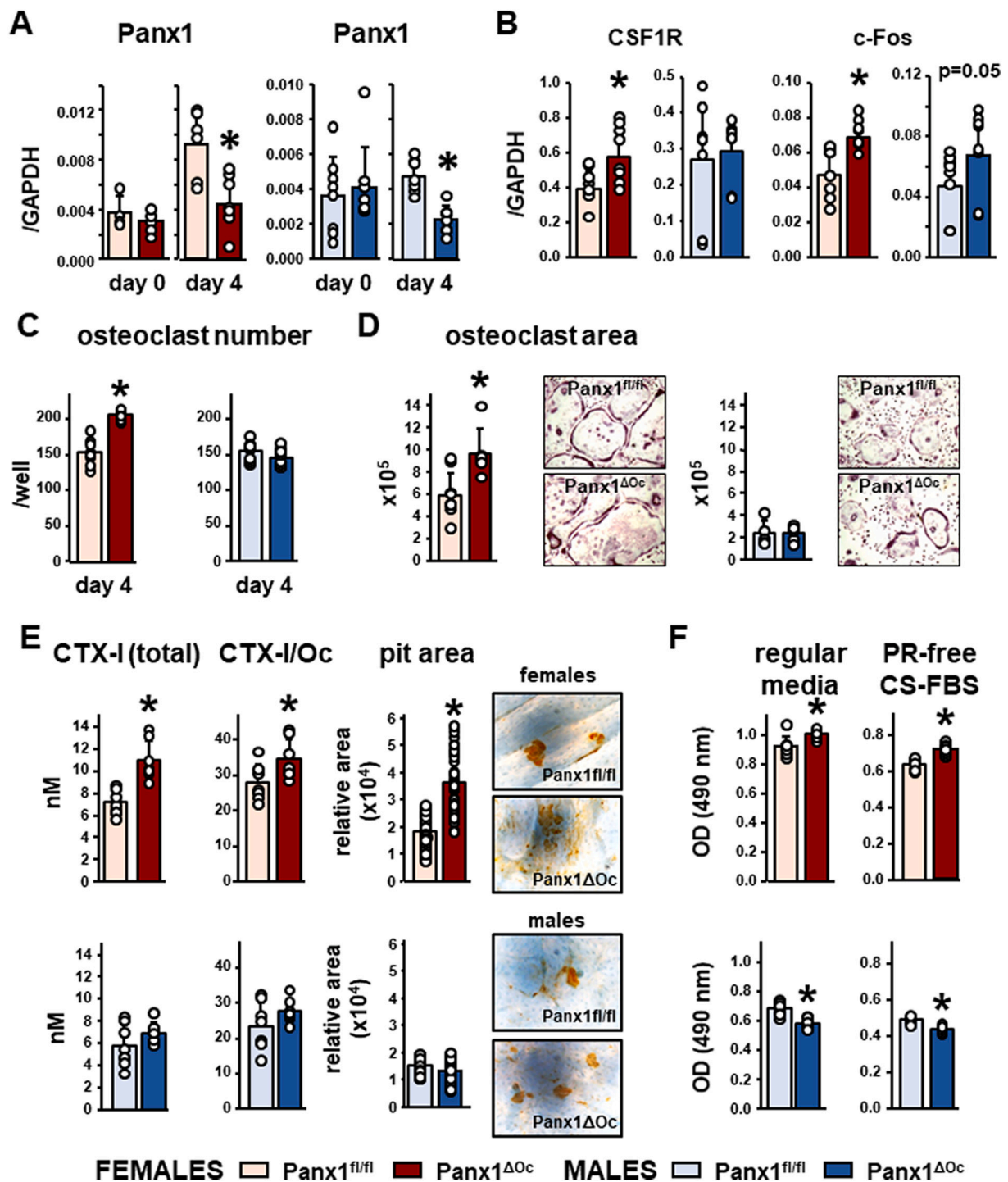


Fig. 5. High osteoclastogenic potential and increased activity of osteoclastic cells derived from female Panx1-deficient mice. **A.** Panx1 expression in cells isolated from 6-week-old mice at the time of seeding and after 4 day-treatment with M-CSF/RANKL. **B.** Gene expression in bone marrow cells cultured for 4 days under osteoclastogenic conditions. **C** and **D** osteoclast number and area of *ex vivo* osteoclasts cultured for 4 days on plastic. Images are representative of osteoclast cultures. **E.** CTX-I levels in the media measured/well (total) or corrected by the number of osteoclasts, and relative pit area of *ex vivo*-generated osteoclasts cultured for 3 days on bone slices. **F.** Non-adherent bone marrow cells were cultured in the presence of regular media or with phenol red-free (PR-free) α -MEM supplemented with charcoal-stripped fetal bovine serum (CS-FBS) for 3 days. $N = 8$ /group for A-E, 4/group for F. Bars indicate means and lines standard deviations, and each dot corresponds to an individual sample. *: $p < 0.05$ vs. Panx1^{fl/fl} mice for the same sex.

4. Discussion

Work from our laboratory has demonstrated that deletion of Panx1 channels from osteocytic cells results in sex-specific effects on bone and skeletal muscle (Aguilar-Perez et al., 2019). We now report that, deletion of Panx1 in TRAP-expressing cells results in decreased bone mass in

males and females but, similar to the effects of osteocytic deletion of Panx1 (Aguilar-Perez et al., 2019), deletion of osteoclastic Panx1 has sex-dependent consequences. Thus, female Panx1^{ΔOc} mice exhibit high osteoclast-related parameters *in vivo*, and osteoclast differentiation and activity are higher in cells isolated from Panx1-deficient mice compared to Panx1^{fl/fl} littermate controls. On the other hand, although osteoclasts

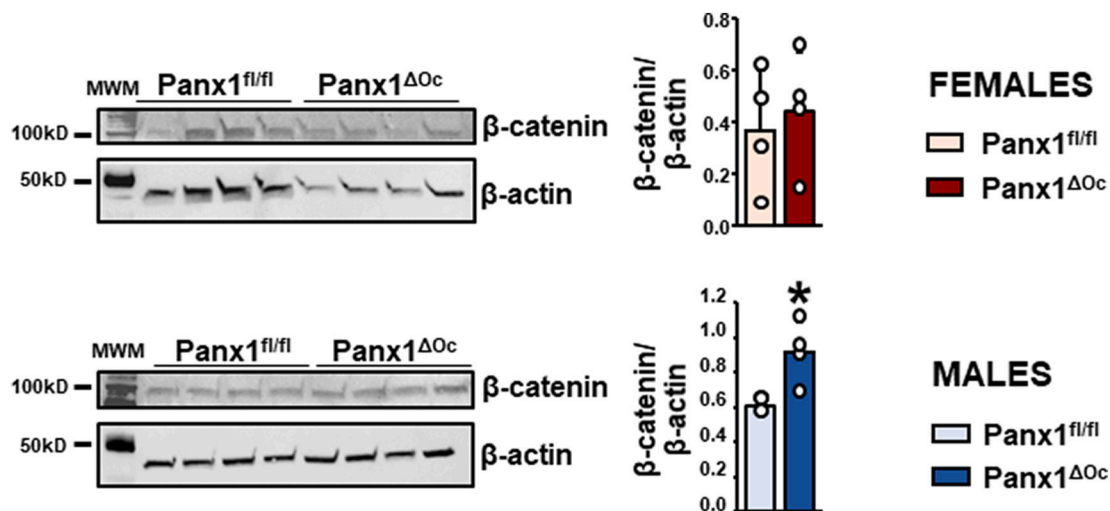


Fig. 6. β -catenin accumulates in osteoclasts derived from male, but not female, $Panx1^{\Delta Oc}$ mice. Protein lysates were obtained from osteoclastic cells generated by treatment with M-CSF/RANKL for 4 days. Proteins were separated by SDS-PAGE, transferred to PVDF membranes, and probed for β -catenin and β -actin as house-keeping gene. Images were quantified using Image J and the densitometric values for β -catenin were divided by β -actin for the same sample. $N = 4$ /group. Bars indicate means and lines standard deviations, and each dot corresponds to an individual sample. *: $p < 0.05$ vs. $Panx1^{fl/fl}$ mice for the same sex.

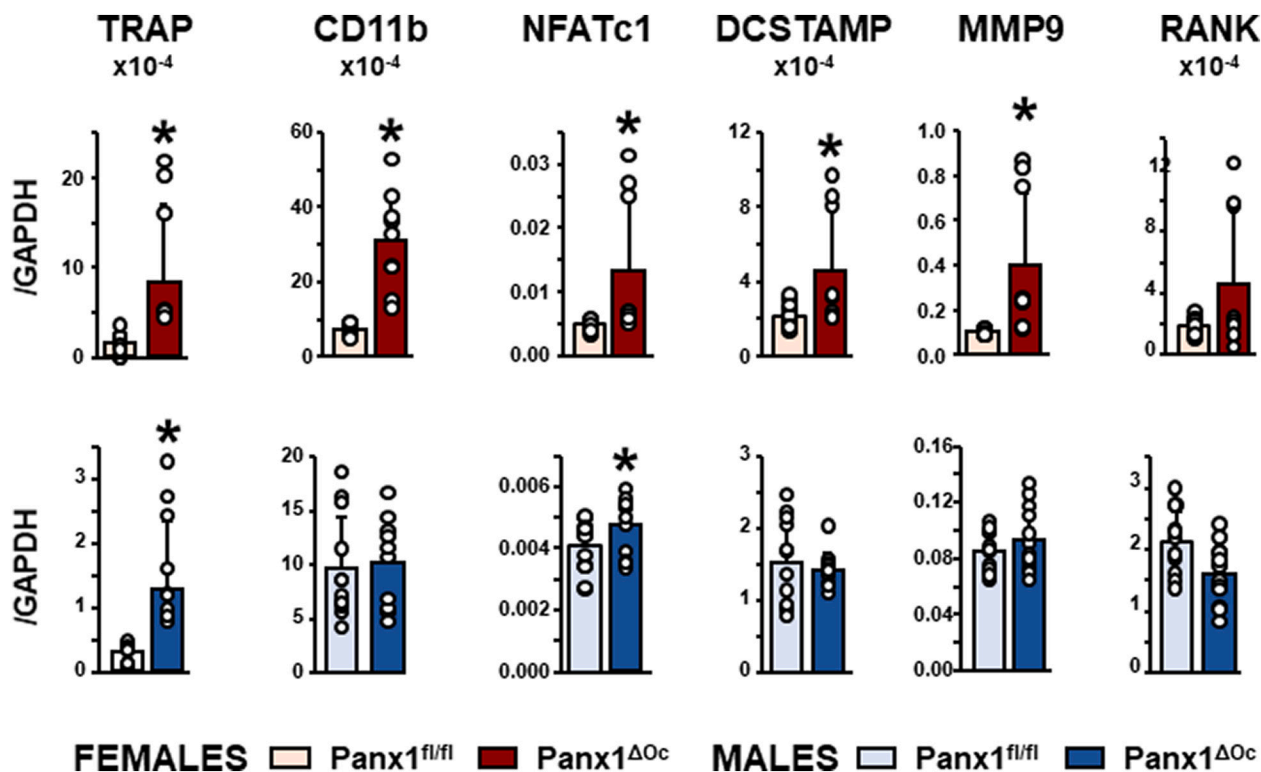


Fig. 7. Increased expression of osteoclast-related genes in vertebral bone from $Panx1$ -deficient mice. The sixth lumbar vertebra was isolated from 6-week-old mice, and the level of the indicated genes was measured by qPCR and corrected by GAPDH as the housekeeping gene. $N = 9-12$ /group. Bars indicate means and lines standard deviations, and each dot corresponds to an individual sample. *: $p < 0.05$ vs. $Panx1^{fl/fl}$ mice for the same sex.

are minimally affected in male $Panx1^{\Delta Oc}$ mice, osteoblast activity is decreased *ex vivo* and *in vivo* (Fig. 9).

Our study showed an unexpected consequence of osteoclastic $Panx1$ deletion. In female mice, deletion of the gene has a direct effect on osteoclasts increasing their differentiation *ex vivo* and activity *in vitro* and *in vivo*. On the other hand, minimal effects were observed in $Panx1^{\Delta Oc}$ male osteoclast progenitors, without altered bone resorption. Instead, changes in the osteoclast secretome – even in the absence of bone resorption in cells cultured on plastic – causes reduction in osteoblast

mineralization from cells exposed to the CM from $Panx1^{\Delta Oc}$ osteoclasts. A potential candidate to explain this observation is ATP, known to be released to the extracellular space *via* pannexin channels. Although still controversial, studies have shown that ATP may synergize with phosphatases to induce osteoblastic cell mineralization (Agrawal and Jorgensen, 2021). However, we cannot rule out the possibility that small peptides or cleavage products are released through $Panx1$ channels, or that channel independent functions of the pannexin are involved in the observed phenotype. Whether this is the case in our system, and the

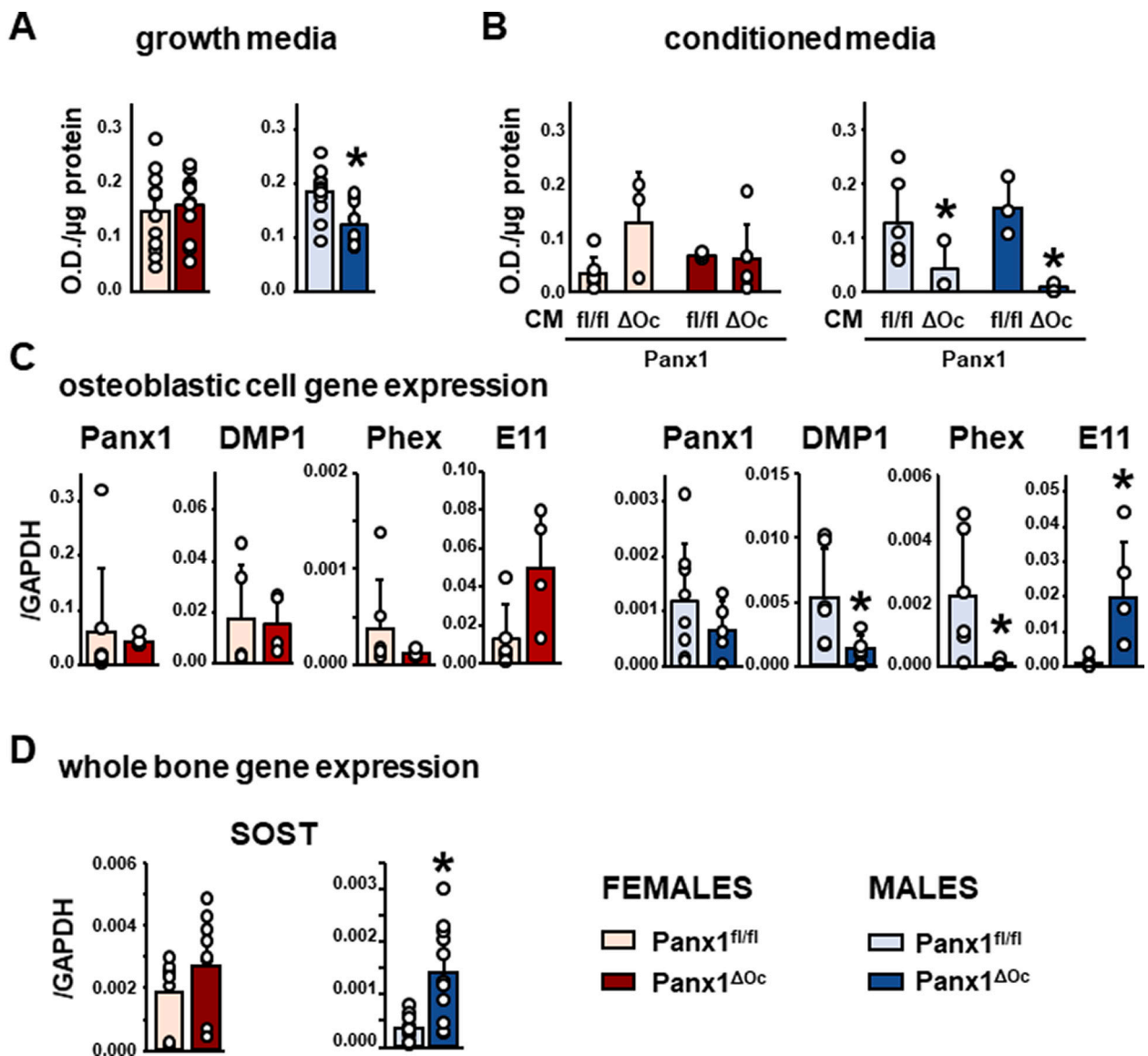


Fig. 8. Reduced mineralization in Panx1-deficient male mice. A-B. *Ex vivo* mineralization assay of bone marrow stromal cells cultured in osteoblastogenic media alone (A), or with conditioned media from osteoclasts of either genotype and the same sex (B). C. Gene expression in stromal osteoblastic cells treated for 14 days with osteoblastogenic media. D. Sost expression in the sixth lumbar vertebra from Panx1^{ΔOc} mice and Panx1^{fl/fl} littermate controls. N = 3–12 /group (A-B), 4–8 (C), or 9–12 (D). Bars indicate means and lines standard deviations, and each dot corresponds to an individual sample. *: p < 0.05 vs. Panx1^{fl/fl} mice for the same sex.

reason why this only happens when osteoclasts are derived from male mice remains to be investigated.

Another original finding of our studies is the effect on osteoblastic cells only seen in Panx1^{ΔOc} male mice. The reduced mineralization combined with the increased E11/podoplanin and Sost levels, and the decreased osteoid in vertebrae raise the possibility that removal of Panx1 results in changes in the osteoclast secretome, leading to accelerated osteocytogenesis. Thus, either the absence or presence of a factor released by osteoclasts, or secreted only in the absence of Panx1, leads to changes in mesenchymal stem cell progenitors that might accelerate the differentiation of osteoblastic precursors. We propose that Panx1 deletion thereby leads to a reduction in the time in which the cells induce bone mineralization – while at the same time decreasing the expression of genes associated with bone mineralization such as DMP1 and Phex (Bellido et al., 2019) – and increasing their terminal differentiation into osteocytes. The validity of this hypothesis and the mechanism by which this effect is only present in male mice, remain to be investigated.

Pannexins oligomerize to form channels on the cell membrane (Penuela et al., 2012). Unlike connexin channels, which exhibit similar

structures, pannexin channels do not form gap junctions and are known to mediate the communication of the cells with the extracellular milieu. More recently, work of the Peñuela laboratory demonstrated that Panx1 binds to βcatenin in melanoma cells, a mechanism involved in the regulation of melanoma cell growth and metabolism (Sayedyahosseini et al., 2021), which might be independent of the function of Panx1 as a channel forming protein. Interestingly, whereas the study in melanoma cells (which appear to be originated from female patients) showed reduced βcatenin levels in Panx1-deficient melanoma cells, we found that deletion of Panx1 results in increased βcatenin levels in osteoclasts, albeit only in cells derived from male mice. This evidence suggests that the molecular mechanism of Panx1 action is different in melanoma cells versus osteoclasts.

In summary, we report for the first time a role of Panx1 in osteoclasts that depends on the sex of the mice. Further, we have unveiled a mechanism by which deletion of Panx1 in osteoclasts leads to indirect effects on osteoblasts *in vitro* and *in vivo* (Fig. 9). Although we have shown here that deletion of osteoclastic Panx1 results in changes in osteoclast differentiation and osteoblast mineralization, as well as gene

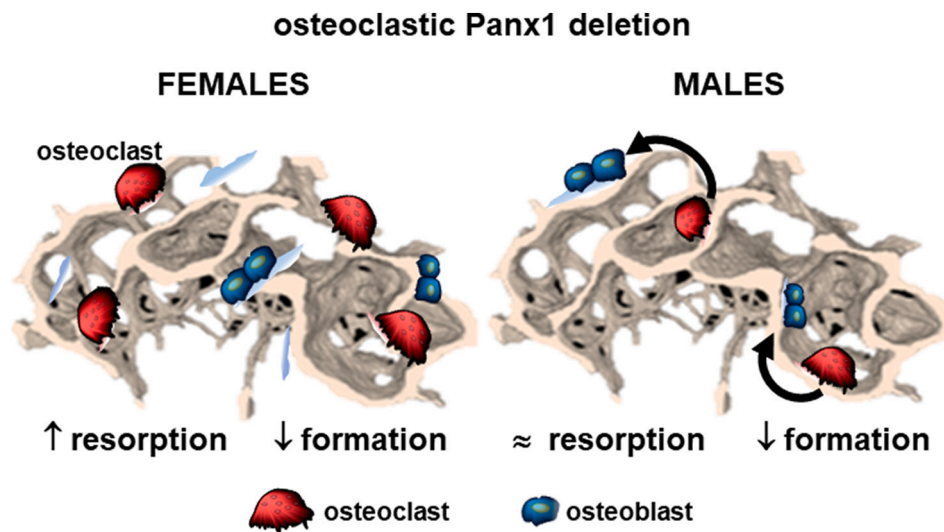


Fig. 9. Osteoclastic Panx1 deletion results in differential effects on bone cells in female and male Panx1^{ΔOC} mice. Schematic representation of the findings reported in this manuscript, with higher resorption in females and reduced formation in both males and females, resulting in reduced cancellous bone mass in 6-week-old growing mice. We hypothesize that, whereas the consequences of osteoclastic Panx1 deletion are primarily cell autonomous, the reduction in bone mass in male mice results from an altered osteoclast secretome leading to reduced osteoblast activity.

expression *ex vivo* and *in vivo* in young mice, the mechanisms for the sex-specific effects of the channel are not completely understood. Thus, future studies are needed to further understand the molecular basis of the observed phenotypes, and whether the consequences of Panx1 deletion are maintained, exacerbated, or abolished with aging.

CRedit authorship contribution statement

Padmini Deosthale: Investigation, Formal analysis, Writing – original draft, Writing – review & editing. **Jung Min Hong:** Investigation, Formal analysis, Writing – review & editing. **Alyson L. Essex:** Investigation, Formal analysis, Writing – review & editing. **Wilyaet Rodriguez:** Investigation, Writing – review & editing. **Dua Tariq:** Investigation, Writing – review & editing. **Harmandeep Sidhu:** Investigation, Writing – review & editing. **Alejandro Marcial:** Investigation, Writing – review & editing. **Angela Bruzzaniti:** Formal analysis, Methodology, Resources, Writing – review & editing. **Lilian I. Plotkin:** Conceptualization, Formal analysis, Writing – original draft, Writing – review & editing.

Declaration of competing interest

The authors declare that they have no known competing financial interests or personal relationships that could have appeared to influence the work reported in this paper.

Acknowledgements

These studies were supported by the National Institutes of Health (RO-AR053643 to LIP) and an ICMH Collaborative Pilot Grant to LIP and AB. ALE received support from the NIH T32-AR065971 grant, WR was supported by the Summer Undergraduate Research Experience in the Biomedical Sciences (SUREBS) at Indiana University School of Medicine, HS was a scholar from Life-Health Sciences Internship Program (LHSI), AM was supported by the Diversity Scholars Research Program (DSRP) and the Indiana University-Purdue University at Indianapolis Undergraduate Research Opportunity Program (IUPUI-UROP), and DT by the Indiana University-Purdue University at Indianapolis Undergraduate Research Opportunity Program (IUPUI-UROP). We thank Dr. Roger J. Thompson (University of Calgary, Alberta, Canada) for providing the protocol for identification of the deleted form of Panx1 and Dr. Kenneth White for providing reagents for qPCR analysis, Dr. Julian Balanta-Melo for help with μ CT images, and Dr. Hannah M. Davis for the bone and bone cell schematic diagram (Indiana University School of Medicine,

Indiana, USA).

References

- Agrawal, A., Jorgensen, N.R., 2021. Extracellular purines and bone homeostasis. *Biochem. Pharmacol.* 187, 114425.
- Aguilar-Perez, A., Pacheco-Costa, R., Atkinson, E.G., Deosthale, P., Davis, H.M., Essex, A. L., et al., 2019. Age- and sex-dependent role of osteocytic pannexin1 on bone and muscle mass and strength. *Sci. Rep.* 9 (1), 13903.
- Bellido, T., Plotkin, L.I., Bruzzaniti, A., 2019. In: Burr, D.B., Allen, M.R. (Eds.), *Basic and Applied Bone Biology*. Elsevier, 125 London Wall, London EC2Y 5AS, United Kingdom, pp. 37–56.
- Beyer, E.C., Berthoud, V.M., 2018. Gap junction gene and protein families: connexins, innexins, and pannexins. *Biochim. Biophys. Acta* 1860 (1), 5–8.
- Bouxein, M.L., Boyd, S.K., Christians, B.A., Guldberg, R.E., Jepsen, K.J., Muller, R., 2010. Guidelines for assessment of bone microstructure in rodents using micro-computed tomography. *J. Bone Miner. Res.* 25 (7), 1468–1486.
- Chiu, W.S., McManus, J.F., Notini, A.J., Cassady, A.I., Zajac, J.D., Davey, R.A., 2004. Transgenic mice that express cre recombinase in osteoclasts. *Genesis* 39 (3), 178–185.
- Davis, H.M., Pacheco-Costa, R., Atkinson, E.G., Brun, L.R., Gortazar, A.R., Harris, J., et al., 2017. Disruption of the Cx43/miR21 pathway leads to osteocyte apoptosis and increased osteoclastogenesis with aging. *Aging Cell* 16 (3), 551–563.
- Davis, H.M., Aref, M.W., Aguilar-Perez, A., Pacheco-Costa, R., Allen, K., Valdez, S., et al., 2018. Cx43 overexpression in osteocytes prevents osteocyte apoptosis and preserves cortical bone quality in aging mice. *JBMR Plus*. <https://doi.org/10.1002/jbm4.10035>.
- Davis, H.M., Valdez, S., Gomez, L., Malicky, P., White, F.A., Suble, M.A., et al., 2019. High mobility group box1 (HMGB1) protein regulates osteoclastogenesis through direct actions on osteocytes and osteoclasts in vitro. *J. Cell. Biochem.* 120 (10), 16741–16749.
- Davis, H.M., Essex, A.L., Valdez, S., Deosthale, P.J., Aref, M.W., Allen, M.R., et al., 2019. Short-term pharmacologic RAGE inhibition differentially affects bone and skeletal muscle in middle-aged mice. *Bone* 124, 89–102.
- Davis, H.M., Deosthale, P.J., Pacheco-Costa, R., Essex, A.L., Atkinson, E.G., Aref, M.W., et al., 2020. Osteocytic miR21 deficiency improves bone strength independent of sex despite having sex divergent effects on osteocyte viability and bone turnover. *FEBS J.* 287 (5), 941–963.
- Dempster, D.W., Compston, J.E., Drezner, M.K., Glorieux, F.H., Kanis, J.A., Malluche, H., et al., 2013. Standardized nomenclature, symbols, and units for bone histomorphometry: a 2012 update of the report of the ASBMR histomorphometry nomenclature committee. *J. Bone Miner. Res.* 28 (1), 2–17.
- Kang, K.S., Hong, J.M., Horan, D.J., Lim, K.E., Bullock, W.A., Bruzzaniti, A., et al., 2019. Induction of Lrp5 HBM-causing mutations in cathepsin-K expressing cells alters bone metabolism. *Bone* 120, 166–175.
- Kobayashi, Y., Uehara, S., Koide, M., Takahashi, N., 2015. The regulation of osteoclast differentiation by wnt signals. *Bonekey Rep.* 4, 713.
- Li, L., Wang, B., Li, Y., Li, L., Dai, Y., Lv, G., et al., 2020. Celastrol regulates bone marrow mesenchymal stem cell fate and bone-fat balance in osteoporosis and skeletal aging by inducing PGC-1 α signaling. *Aging (Albany NY)* 12 (17), 16887–16898.
- Livak, K.J., Schmittgen, T.D., 2001. Analysis of relative gene expression data using real-time quantitative PCR and the 2- $\Delta\Delta$ CT method. *Methods* 25 (4), 402–408.
- Mohamad, S.F., Xu, L., Ghosh, J., Childress, P.J., Abeysekera, I., Himes, E.R., et al., 2017. Osteomacs interact with megakaryocytes and osteoblasts to regulate murine hematopoietic stem cell function. *Blood Adv.* 1 (26), 2520–2528.

- Mohamad, S.F., Gunawan, A., Blosser, R., Childress, P., Aguilar-Perez, A., Ghosh, J., et al., 2021. Neonatal osteomacs and bone marrow macrophages differ in phenotypic marker expression and function. *J. Bone Miner. Res.* 36 (8), 1580–1593.
- Otsu, N., 1979. A threshold selection method from gray level histograms. *IEEE Trans. Syst. Man Cybern.* 9 (1), 62–66.
- Pacheco-Costa, R., Davis, H.M., Atkinson, E.G., Dilley, J.E., Byiringiro, I., Aref, M.W., et al., 2018. Reversal of loss of bone mass in old mice treated with mefloquine. *Bone* 114, 22–31.
- Penuela, S., Gyenis, L., Ablack, A., Churko, J.M., Berger, A.C., Litchfield, D.W., et al., 2012. Loss of pannexin 1 attenuates melanoma progression by reversion to a melanocytic phenotype. *J. Biol. Chem.* 287 (34), 29184–29193.
- Plotkin, L.I., Bellido, T., 2016. Osteocytic signalling pathways as therapeutic targets for bone fragility. *Nat. Rev. Endocrinol.* 12 (10), 593–605.
- Plotkin, L.I., Davis, H.M., Cisterna, B.A., Saez, J.C., 2017. Connexins and pannexins in bone and skeletal muscle. *Curr. Osteoporos. Rep.* 15 (4), 326–334.
- Posritong, S., Hong, J.M., Eleniste, P.P., McIntyre, P.W., Wu, J.L., Himes, E.R., et al., 2018. Pyk2 deficiency potentiates osteoblast differentiation and mineralizing activity in response to estrogen or raloxifene. *Mol. Cell. Endocrinol.* 474, 35–47.
- Sayed-yahosseini, S., Huang, K., Li, Z., Zhang, C., Kozlov, A.M., Johnston, D., et al., 2021. Pannexin 1 binds beta-catenin to modulate melanoma cell growth and metabolism. *J. Biol. Chem.* 100478.
- Weivoda, M.M., Ruan, M., Hachfeld, C.M., Pederson, L., Howe, A., Davey, R.A., et al., 2016. Wnt signaling inhibits osteoclast differentiation by activating canonical and noncanonical cAMP/PKA pathways. *J. Bone Miner. Res.* 31 (1), 65–75.
- Wu, J.L., McIntyre, P.W., Hong, J.M., Yassen, G.H., Bruzzaniti, A., 2020. Effects of radiopaque double antibiotic pastes on the proliferation, alkaline phosphatase activity and mineral deposition of dental pulp stem cells. *Arch. Oral Biol.* 117, 104764.